

Lifetime measurements in the regular  $\Delta I = 1$  oblate band in  $^{197}\text{Pb}$ 

J. R. Hughes, J. A. Becker, M. J. Brinkman, E. A. Henry, R. W. Hoff, M. A. Stoyer, and T. F. Wang  
Lawrence Livermore National Laboratory, Livermore, California 94550

B. Cederwall, M. A. Deleplanque, R. M. Diamond, P. Fallon, I. Y. Lee, J. R. B. Oliveira, and F. S. Stephens  
Lawrence Berkeley Laboratory, Berkeley, California 94720

J. A. Cizewski and L. A. Bernstein  
Rutgers University, New Brunswick, New Jersey 08903

J. E. Draper, C. Duyar, and E. Rubel  
Physics Department, University of California, Davis, California 95616

W. H. Kelly and D. Vo  
Iowa State University, Ames, Iowa 50010  
(Received 23 July 1993)

Lifetimes of states in the regular  $\Delta I = 1$  band in  $^{197}\text{Pb}$  have been measured with the Doppler-shift attenuation method. Excited states in  $^{197}\text{Pb}$  were populated using the  $^{154}\text{Sm}(^{48}\text{Ca}, 5n)$  reaction at  $E_b = 210$  MeV. The target consisted of  $1 \text{ mg/cm}^2$   $^{154}\text{Sm}$  evaporated onto a  $10 \text{ mg/cm}^2$  Au backing. Discernible lineshapes for  $\gamma$  rays in the energy range  $300 < E_\gamma < 500$  keV in the regular band were observed in a spectroscopic study with the 20 Ge-detector array, HERA. Level lifetimes were obtained from a lineshape analysis. Averaged reduced transition strengths,  $B(M1) \sim 1.7$  W.u. and  $B(E2) \sim 18$  W.u., are deduced and these are compared with theoretical predictions for the suggested configuration of this band.

PACS number(s): 21.10.Re, 21.10.Tg, 21.60.Ev, 27.80.+w

The neutron-deficient Pb isotopes have been the subject of considerable interest recently. Experimental information suggests that in addition to the well-established superdeformed bands, collective excitations may also occur in the first well of these singly magic nuclei. Specifically, a number of "regular" and "irregular" dipole bands have been observed at higher angular momentum ( $I \sim 20\hbar$ ) and excitation energy ( $E_x \sim 4\text{--}5$  MeV) in both the even  $^{192\text{--}200}\text{Pb}$  [1–8] and odd  $^{197\text{--}201}\text{Pb}$  [8–11] nuclei. In contrast, the low-spin excitations of these nuclei can be described in terms of single-particle degrees of freedom [12].

The regular  $\Delta I=1$  bands are generally characterized by large  $B(M1)/B(E2)$  ratios, small dynamic moments of inertia,  $\mathcal{J}^{(2)}$ , and very little signature splitting. These experimental features are similar to those found in the oblate bands in the  $A \sim 130$  mass region [13]. The regular bands in both regions have generally been interpreted as collective oblate rotational structures. However, without lifetime measurements the collectivity remains undetermined. Lifetime measurements also provide important information regarding the single-particle structure involved. The microscopic configuration of these bands in the Pb nuclei is thought to involve quasiproton excitations across the spherical  $Z = 82$  shell gap, coupled to a number of rotation-aligned high- $j$  quasineutrons. The suggested quasiproton structure is similar to that responsible for the  $11^-$  isomeric states observed in some of the even Pb isotopes [14].

Measured  $M1$  transition rates for these bands are only available in  $^{198}\text{Pb}$  [6], where the  $B(M1)$  values are as

strong as any yet observed in heavy nuclei. The  $B(E2)$  values derived from the branching ratios suggest a small quadrupole moment and deformation ( $\beta_2 \sim 0.1$ ). The present Rapid Communication reports on lifetime measurements in the previously observed [9,10] regular dipole band of  $^{197}\text{Pb}$ . These measurements represent the second such example in the dipole bands of this mass region, and the first in an odd- $A$  nucleus. A preliminary report of this work has been presented previously [15].

Excited states in  $^{197}\text{Pb}$  were populated using the  $^{154}\text{Sm}(^{48}\text{Ca}, 5n)$  reaction at a beam energy  $E_i = 210$  MeV. The target consisted of  $1 \text{ mg/cm}^2$   $^{154}\text{Sm}$  evaporated onto a  $10 \text{ mg/cm}^2$  Au backing. The in-beam  $\gamma$  rays were detected using the HERA spectrometer at the Lawrence Berkeley Laboratory 88-Inch Cyclotron Facility. The measurements described here were performed with 20 Compton-suppressed germanium detectors together with a 40-element bismuth-germanate (BGO) inner ball. The number of Ge detectors at each angle with respect to the beam direction ( $n, \theta$ ) is (4,  $37^\circ$ ), (2,  $51^\circ$ ), (4,  $79^\circ$ ), (2,  $103^\circ$ ), (4,  $123^\circ$ ), (2,  $152^\circ$ ), and (2,  $154^\circ$ ). Each detector is 15.5 cm from the target and subtends  $\sim 82$  msr. All three- and higher-fold events were recorded, together with sum-energy and multiplicity information. Twofold events were recorded only if four or more inner BGO elements were in prompt coincidence. The data set consists of approximately  $3.0 \times 10^8$  expanded twofold events with these requirements.

The previously observed [9,10] band structures in  $^{197}\text{Pb}$  are prominent in the present data set: the regular dipole band is shown in Fig. 1. Our analysis confirms the

level ordering, and the placement of the 371-keV transition by Clark *et al.* [10], although the 415-keV transition is too weak in our data for verification. We are also able to confirm the previous report [16] that  $\sim 50\%$  of the decay of the regular band proceeds through the 50 ns isomeric ( $33/2^+$ ) state. This state is interpreted as  $\nu(i_{13/2})^3$  [17].

In order to facilitate the lineshape analysis, the data were sorted into three asymmetric matrices consisting of coincidences between events in (1) detectors at  $37^\circ$  with any detector (backward versus all), (2) detectors at  $79^\circ$  and  $103^\circ$  with any detector (transverse versus all), and (3) detectors at  $152^\circ$  and  $154^\circ$  with any detector (forward versus all). In each case, a minimum inner ball fold of 6 was required. A lineshape analysis was performed on summed spectra which were obtained with gates set on fully stopped in-band transitions on the “all” axis of each matrix. Lineshapes were observed for the in-band  $\Delta I = 1$  transitions in the energy range  $300 < E_\gamma < 500$  keV; level lifetimes were extracted from these using the

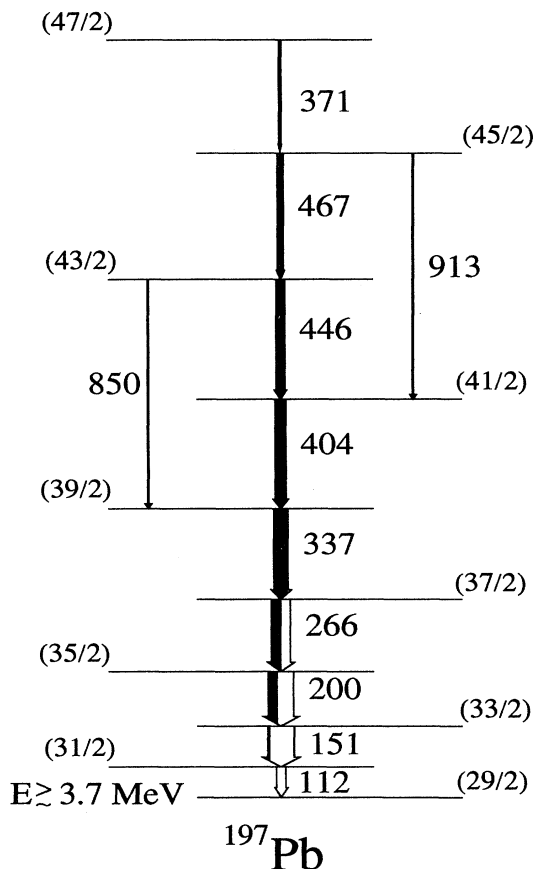


FIG. 1. Partial level scheme for  $^{197}\text{Pb}$ , showing the regular dipole band as observed by [9,10]. Arrow widths represent total transition intensities, with the relative  $\gamma$ -ray intensity represented by the shaded part. The transition intensities of the two lowest band members have large errors due to the low  $\gamma$ -ray intensity (high internal conversion), and uncertainties in the coincidence efficiency. Tentative spins are given for the levels, and a minimum excitation energy for the lowest band member is given.

code DSAMFT\_OR [18]. Nuclear and electronic stopping powers were calculated using the compilation of Ziegler *et al.* [19]. The detailed slowing-down history of  $^{197}\text{Pb}$  recoils in the target and backing material was simulated using Monte Carlo techniques (5000 histories with a time step of 0.002 ps), and then sorted according to the detector geometry. Calculated lineshapes for each in-band transition were obtained assuming both (1) a precursor cascade of rotational transitions feeding the top of the band, and (2) side feeding into each state modeled by a cascade of five transitions, with a moment of inertia similar to the main cascade. The intensity of the side feeding was constrained to reproduce that observed experimentally. Simultaneous fits to the forward, backward, and transverse spectra were made. The transverse spectra proved important for the identification of contaminant lines.

Final results were obtained from a global fit to the whole band, with independently variable lifetimes for each state and associated side-feeding band. The experimental data obtained for the 404- and 446-keV  $\Delta I = 1$  transitions at forward and backward angles, along with the corresponding fits, are shown in Fig. 2. The results obtained from this lineshape analysis are summarized in Table I. The listed errors do not include those associated with the stopping powers, which may be as large as  $\pm 20\%$ . The lifetimes extracted for a number of states in the regular band in  $^{197}\text{Pb}$  are listed together with the corresponding reduced transition probability,  $B(M1)$ , deduced with the assumption that the multipole mixing ratio,  $\delta = 0$ , and using the spins given in Fig. 1. The  $B(M1)$  values are large, with an average of  $1.7(5)$  W.u. Best fits were obtained with side-feeding lifetimes approximately 25–40% greater than those for the in-band transitions. The regular band in  $^{197}\text{Pb}$  is also weakly populated in the  $^{198}\text{Pb}$  data set of Wang *et al.* [6]. We have been able to extract a lifetime for one of the states in the regular band of  $^{197}\text{Pb}$  from the data of Wang *et al.* obtained with a Pb-backed target. The value obtained (see Table I) is in good agreement with that obtained from the present Au-backed  $^{197}\text{Pb}$  data set (the stopping times in Au and Pb backings differ by a factor  $\sim 2$ ). Unfortunately, the lifetimes of other states in the regular band could not be extracted from the Pb-backed target data due to strong contaminant lines.

The  $B(E2)$  values are listed for states where the  $E2/M1$   $\gamma$ -ray branching ratio is experimentally known. From the averaged  $B(E2)$  values, the transition quadrupole moment can be extracted [ $Q_t = 3.0(12)$  e b], leading to a model-dependent [20] estimate for the quadrupole deformation,  $\beta_2 = 0.10(4)$ . It is apparent from the decay sequence (Fig. 1), and the  $\mathcal{J}^{(2)}$  values that the band is undergoing an upbend in the region where the  $E2$  transitions are observed. This may result in lower  $B(E2)$  values than those above or below the upbend [21].

The extracted  $B(M1)$  and  $B(E2)$  values are comparable to those obtained from a similar study of  $^{198}\text{Pb}$  [6]. The differences in the systematic errors between these two data sets are expected to be small since the same reaction and target material were used in both. The

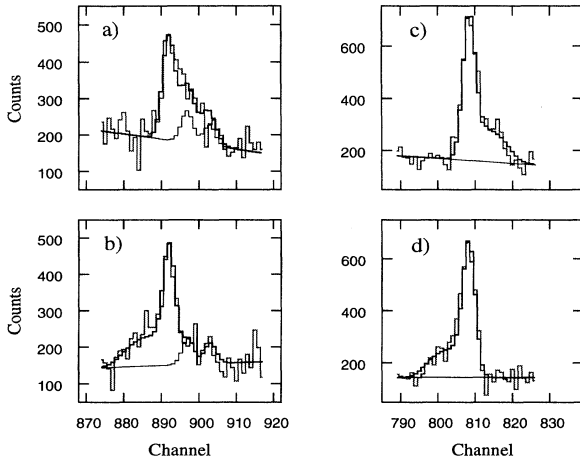


FIG. 2. DSAM fits to selected transitions in the regular band of  $^{197}\text{Pb}$ . The data are shown in gray, background and contaminant lines in thin black, and the total fit is shown in thick black for (a) the 446-keV transition, forward angles, and (b) backward angles spectrum, and (c) the 404-keV transition, forward, and (d) backward spectrum.

$B(M1)$  values in  $^{197}\text{Pb}$  show little variation with increasing spin, as was found for band I in  $^{198}\text{Pb}$ , but the  $^{197}\text{Pb}$  values are slightly larger in magnitude. The suggested configuration for these two bands is similar, with the exception of the additional quasineutron in  $^{197}\text{Pb}$ .

In the following, the results obtained for  $^{197}\text{Pb}$  will be compared to theoretical predictions for the  $M1$  reduced transition probability using the geometrical model of Dönau and Frauendorf [22], in order to investigate the microscopic structure of this band. The extracted quadrupole deformation will be compared to the results of cranked-shell-model (CSM) and total-Routhian-surface (TRS) [26] calculations. Based on the available spectroscopic information, the suggested configuration for the regular band in  $^{197}\text{Pb}$  is  $\pi(i_{13/2} \otimes h_{9/2})_{K^\pi=11^-} \otimes \nu(i_{13/2})^3$  [9]. The calculations presented below have been performed for this, and other configurations containing high- $K$  quasiproton excitations.

The large magnitudes of the extracted  $B(M1)$  values are consistent with the suggestion that quasiproton excitations are present in the microscopic structure of this band. The relatively small  $\mathcal{J}^{(2)}$  ( $\sim 17\hbar^2/\text{MeV}$ ) suggests that a pair of rotation-aligned high- $j$  quasineutrons (along with the odd quasineutron) are also involved.

An estimate of the  $B(M1)$  for the  $\pi(i_{13/2} \otimes h_{9/2})_{K^\pi=11^-} \otimes \nu(i_{13/2})^3$  configuration taking both neutron and proton contributions into account, may be obtained from the Dönau and Frauendorf formula [22]. One obtains  $B(M1) \sim 4.5$  W.u. at  $I = 24$ . This estimate is obtained using  $g_K = 0.96$  for the  $\pi(i_{13/2} \otimes h_{9/2})_{K^\pi=11^-}$  configuration, and  $g_K = -0.15$  for the  $(i_{13/2})^3$  quasineutrons. These  $g_K$  values are those extracted experimentally for the  $g$  factors of the  $11^-$  state in  $^{196}\text{Pb}$  [23], and the  $(33/2^+)$  state in  $^{197}\text{Pb}$  [17]. The summed alignments ( $\pi i_x = 4.0\hbar$ ,  $\nu i_x = 16\hbar$ , at  $\hbar\omega = 0.25$  MeV) used have been extracted for the relevant orbitals from CSM results (see below).

Similar large  $B(M1)$  values are also predicted when quasiproton excitations occupy other combinations of high- $j$  orbitals located near the Fermi surface. For instance, the  $\pi(h_{9/2})_{K^\pi=8^+}$  excitation, responsible for the  $8^+$  isomeric state observed in, for example,  $^{196}\text{Pb}$  could give rise to coupled bands of  $M1$  transitions (the  $K^\pi = 0^+$  coupling is not expected to produce such structures). The experimentally derived  $B(M1)$  values along with a number of calculated values, appropriate for different quasiproton configurations, are shown in Fig. 3. The errors shown on the calculated values are dominated by uncertainties in the  $K$  value [ $B(M1)_{DF} \sim K^2$ ], but also contain the errors associated with uncertainties in the spin assignments, and alignments. These errors do not, however, contain the errors in the  $g_K$  values, which may be large.

The calculated quasiproton configurations correspond to those responsible for the  $8^+$  and  $11^-$  isomeric states observed in some of the even Pb isotopes [14], and a  $K = 12$  state based on an unobserved  $\pi(i_{13/2})^2$  excitation. The predicted values for the  $\pi(i_{13/2} \otimes h_{9/2}) \otimes \nu(i_{13/2})^3$ , and  $\pi(i_{13/2})^2 \otimes \nu(i_{13/2})^3$ , are larger than those extracted from these lifetime measurements, whereas that for the  $\pi(h_{9/2})^2 \otimes \nu(i_{13/2})^3$  configuration is somewhat smaller.

TABLE I. Lineshape results for the regular band in  $^{197}\text{Pb}$ . The extracted lifetimes are given for the state, along with the energy of the deexciting  $\gamma$  ray. Reduced transition probabilities,  $B(M1)$ , (in Weisskopf units) are quoted assuming  $\delta = 0$  and the spins listed in Fig. 1. Where available, known  $\gamma$ -ray branching ratios are used to deduce  $B(E2)$  values, quoted in Weisskopf units.

$E_\gamma$ (keV)	$\tau$ (ps)	$B_\gamma$ <sup>a</sup>	$B(M1)$ ( $\mu_N^2$ )	$B(M1)$ (W.u.)	$B(E2)$ (W.u.)
337	0.42(12)	b	2.8(8)	1.6(5)	
404	0.21(5)	b	3.6(9)	2.0(5)	
	0.26(7) <sup>c</sup>		2.9(8)	1.6(4)	
446	0.12(6)	0.85(16)	3.9(2.1)	2.2(1.2)	
850		0.15(5)			34(20)
467	0.20(5)	0.82(16)	2.5(6)	1.4(4)	
913		0.18(6)			12(5)
371	0.36(13)	b	2.4(8)	1.3(4)	

<sup>a</sup>  $B_\gamma = I_\gamma / \sum_{\gamma'} I_{\gamma'}$ , where  $I_\gamma$  is the  $\gamma$ -ray intensity.

<sup>b</sup>  $E2$  branch not observed.

<sup>c</sup> Lifetime extracted from the Pb-backed target data set (see text for details).

The principal difference between the calculated  $B(M1)$  values is due to the different  $g$  factors of the  $\pi i_{13/2}$  and  $\pi h_{9/2}$  orbitals, and the different  $K$  values for these configurations. Although the experimental  $B(M1)$  is somewhat lower than that predicted for the suggested configuration, it is difficult to determine precisely from these lifetime data which proton configuration is involved in the structure of the regular band.

The interpretation of this band involves deformation-aligned high- $K$  quasiprotons and rotation-aligned high- $j$  quasineutrons, suggesting that the tilted axis cranking (TAC) Model [24] is appropriate for this band. The TAC model predicts decreasing  $B(M1)$  values with increasing spin, in general, as does the geometrical model [22]. However, the TAC model does give rise to smaller  $B(M1)$  values than those in the geometrical model since the tilting of the quasiparticle angular momenta toward the spin axis reduces the perpendicular component of the magnetic moment [25]. TAC calculations of the  $B(M1)$  values in  $^{198}\text{Pb}$  have been presented by Frauendorf [24]. The values show a decrease relative to the geometrical model, but still overpredict the measured values [6] for both bands, when attenuated Schmidt values are used for the  $g$  factors. Although a detailed TAC calculation is beyond the scope of this paper, the  $B(M1)$  values in  $^{197}\text{Pb}$  are expected to be similar to those in  $^{198}\text{Pb}$ , since the proton configuration is thought to be the same, and the effect of the additional neutron ( $E$  in Ref. [24]) on the  $B(M1)$  is small [25]. In this case, the TAC model predicts  $\sim 40\%$  lower  $B(M1)$  values than the geometrical model in  $^{197}\text{Pb}$ , bringing the calculated values closer to the measured values.

Information on the collectivity of the band may be obtained by comparing the derived quadrupole deformation to that extracted from TRS calculations. Based on the results of CSM calculations, we have extracted TRS results [26] with the initial configuration  $\pi(i_{13/2} \otimes h_{9/2}) \otimes \nu i_{13/2}$ , at  $\omega = 0$ . A stable collective-oblate deformation develops at rotational frequencies in excess of  $\omega \sim 0.28$  MeV/ $\hbar$ , following the alignment of the second and third  $i_{13/2}$  quasineutrons.<sup>1</sup> The configuration following this alignment is  $\pi(i_{13/2} \otimes h_{9/2}) \otimes \nu(i_{13/2})^3$ , which is the suggested bandhead for the  $^{197}\text{Pb}$  regular band. The extracted deformations are  $\beta_2 = 0.13$ ,  $\gamma = -70^\circ$  at  $\omega = 0.28$  MeV/ $\hbar$ , and  $\beta_2 = 0.11$ ,  $\gamma = -71^\circ$  at  $\omega = 0.48$  MeV/ $\hbar$  [27].

We have also extracted TRS results appropriate for the  $\pi(i_{13/2})^2 \otimes \nu(i_{13/2})^3$  and  $\pi(h_{9/2})^2 \otimes \nu(i_{13/2})^3$  configurations. The  $\pi(i_{13/2})^2 \otimes \nu i_{13/2}$  configuration produces a minimum at  $\beta_2 = 0.13 - 0.12$ ,  $\gamma = -72^\circ$  for the frequency range  $0.24 < \hbar\omega < 0.48$  MeV. The  $\pi(h_{9/2})^2 \otimes \nu i_{13/2}$  configuration, however, has a minimum ( $\beta_2 \sim 0.08$ ,  $\gamma \sim -85^\circ$ ) which is rather flat in the range  $-120^\circ < \gamma < -60^\circ$ . It appears that occupation of

<sup>1</sup>The  $AB$   $\nu i_{13/2}$  alignment is blocked by the odd quasineutron. CSM calculations, appropriate for the deformations extracted from the TRS calculations, predict  $\omega \sim 0.20$  MeV/ $\hbar$  for the  $BC$   $\nu i_{13/2}$  crossing.

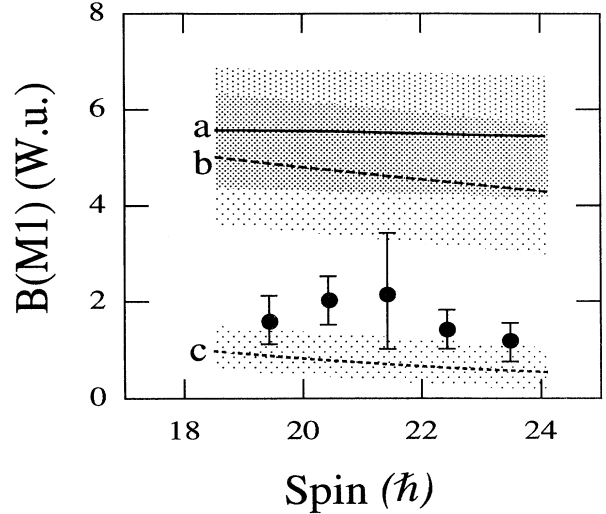


FIG. 3. Experimental and theoretical  $B(M1)$  values. The experimental values, extracted from the Au-backed target data set, are represented by  $\bullet$ . The theoretical values are determined from the geometrical model of Dönau and Frauendorf [22], and correspond to three different quasiproton structures coupled to three rotation-aligned  $i_{13/2}$  quasineutrons: (a)  $\pi(i_{13/2})^2 \otimes \nu(i_{13/2})^3$ , (b)  $\pi(i_{13/2} \otimes h_{9/2}) \otimes \nu(i_{13/2})^3$ , (c)  $\pi(h_{9/2})^2 \otimes \nu(i_{13/2})^3$ . The shading represents the errors associated with the theoretical values.

the  $\pi i_{13/2}$  orbital is needed in order to produce a well-defined minimum in the TRS on the collective oblate axis. The experimentally extracted quadrupole deformation is, however, comparable with those extracted for all three configurations.

It was not possible to extract lifetimes for the states in the irregular band, since the in-band  $\Delta I = 1$  transitions were fully stopped in this data set. It is apparent from the decay sequence that a number of the higher-spin band members are low-energy transitions, possibly with an effective feeding lifetime in excess of the stopping time of the residues in the backing.

In conclusion, the lifetimes of several states in the regular  $\Delta I = 1$  band of  $^{197}\text{Pb}$  have been measured using the DSA method. The  $B(M1)$  values are large [averaging 1.7(5) W.u.] and are similar to those previously observed in  $^{198}\text{Pb}$ . We are unable to uniquely identify the configuration of this band due to uncertainties in the experimental and theoretical values. These large  $B(M1)$  values are, however, consistent with those expected for a high- $K$  configuration containing quasiproton excitations across the spherical  $Z = 82$  shell gap. The  $B(E2)$  values suggest a small quadrupole deformation ( $\beta_2 \sim 0.1$ ), similar to that previously observed in  $^{198}\text{Pb}$ . Calculated deformations for such configurations also indicate small quadrupole deformations. Although the majority of the regular dipole bands in the Pb region have so far been given a collective interpretation, the measured  $B(E2)$  values suggest a small amount of collectivity. It is clear that additional lifetime measurements and theoretical calculations are needed to better understand these bands. Finally, the irregular band members

showed no discernible lineshapes, and so no analysis was attempted for this band.

We thank R. M. Clark and R. Wadsworth for making their RDM results in  $^{197}\text{Pb}$  available prior to publication. We thank the staff of the 88-Inch Cyclotron for flawless operation. The targets were manufactured by Joanne Heagney of MicroMatter Inc. This work was supported in part by U.S. Department of Energy, under Contract No.

W-7405-ENG-48 (LLNL), and No. DE-AC03-76SF00098 (LBL), and in part by the National Science Foundation (Davis, Rutgers), and in part by the Research Corporation Grant No. R-152 and an IPA Independent Research Agreement with the Division of Undergraduate Education of the National Science Foundation (Kelly), the U.S. Department of Energy Division of High Energy and Nuclear Physics under Grants Nos. DE-FG02-92ER40692 and DE-FG02 87ER40371 (ISU).

- 
- [1] M.P. Carpenter *et al.*, Bull. Am. Phys. Soc. **37**, 1285 (1992); E.A. Henry *et al.*, *ibid.* **38**, 1050 (1993); A.J.M. Plompen *et al.*, Nucl. Phys. A (in press).
- [2] B. Fant *et al.*, J. Phys. G **17**, 319 (1991).
- [3] J.R. Hughes *et al.*, Phys. Rev. C **47**, R1337 (1993).
- [4] M.J. Brinkman, Ph.D. thesis, Rutgers University, 1991 (unpublished).
- [5] F. Hannachi *et al.*, in *Proceedings of International Conference in Nuclear Structure at High Angular Momentum*, Ottawa, Canada, 1992 (Report No. AECL-10613, 1992).
- [6] T.F. Wang *et al.*, Phys. Rev. Lett. **69**, 1737 (1992).
- [7] R.M. Clark *et al.*, Phys. Lett. B **275**, 247 (1992).
- [8] G. Baldsiefen *et al.*, Phys. Lett. B **275**, 252 (1992).
- [9] A. Kuhnert *et al.*, Phys. Rev. C **46**, 133 (1992).
- [10] R.M. Clark *et al.*, Z. Phys. A **342**, 371 (1992).
- [11] G. Baldsiefen, H. Hübel, F. Azaiez, C. Bourgeois, D. Hojman, A. Korichi, N. Perrin, and H. Sergolle, Z. Phys. A **343**, 245 (1992).
- [12] K. Honkanen, C.J. Herrlander, B. Fant, and T. Lonroth, Nucl. Phys. **A451**, 141 (1986).
- [13] D.B. Fossan, J.R. Hughes, Y. Liang, R. Ma, E.S. Paul, and N. Xu, Nucl. Phys. **A520**, 241c (1990).
- [14] K. Heyde, P. van Isacker, M. Waroquier, J.L. Wood, and R.A. Meyer, Phys. Rep. **102**, 293 (1983); R. Bengtsson and W. Nazarewicz, Z. Phys. A **334**, 269 (1989).
- [15] J.R. Hughes *et al.*, Bull. Am. Phys. Soc. **38**, 1050 (1993).
- [16] E.A. Henry *et al.*, in [5].
- [17] C. Roulet, G. Albouy, G. Auger, J.M. Lagrange, M. Pautrat, K.G. Rensfelt, H. Richel, H. Sergolle, and J. Vanhorenbeeck, Nucl. Phys. **A285**, 156 (1977); C. Stenzel, H. Grawe, H. Haas, H.-E. Mahnke, and K.H. Maier, Z. Phys. A **322**, 83 (1985).
- [18] DSAMFT.OR, original code by J.C. Bacelar, modified by J. Gascon and J.C. Wells; J.C. Wells (private communication).
- [19] J.F. Zeigler, *The Stopping and Range of Ions in Matter* (Pergamon Press, New York, 1985), Vols. 3 and 5.
- [20] K.E.G. Löbner, M. Vetter, and V. Hönig, Nucl. Data Tables A **7**, 495 (1970).
- [21] J.C. Wells *et al.*, Phys. Rev. C **30**, 1532 (1984).
- [22] F. Dönau and S. Frauendorf, in *Proceedings of the Conference on High Angular Momentum Properties of Nuclei*, Oak Ridge, 1982, edited by N.R. Johnson (Harwood Academic, New York, 1983), p. 143; F. Dönau, Nucl. Phys. **A471**, 469 (1987).
- [23] J. Penninga, W.H.A. Hesselink, A. Balanda, A. Stolk, H. Verheul, J. Van Klinken, H.J. Riezebos, and M.J.A. de Voigt, Nucl. Phys. **A471**, 535 (1987).
- [24] S. Frauendorf, Nucl. Phys. **A 557**, 259c (1993).
- [25] S. Frauendorf (private communication).
- [26] R. Wyss, W. Satula, W. Nazarewicz, and A. Johnson, Nucl. Phys. **A511**, 324 (1990).
- [27] Previous TRS results for this configuration [9] gave similar deformations for the minima, but excitation energies approximately 2 MeV higher than those of the present results. This may be attributed to the inclusion of "hole" excitations in the previous calculations.